Scattering-theory analysis of waveguide-resonator coupling

Yong Xu, Yi Li, Reginald K. Lee, and Amnon Yariv
Department of Applied Physics, California Institute of Technology, MS 128-95, Pasadena, California 91125
(Received 14 May 2000)

Using a formalism similar to the quantum scattering theory, we analyze the problem of coupling between optical waveguides and high Q resonators. We give the optical transmission and reflection coefficients as functions of the waveguide-resonator coupling, cavity loss (gain), and cavity resonant frequency. Based on these results, the recently proposed concept of ''critical coupling'' is discussed. Using a matrix formalism based on the scattering analysis, we find the dispersion relation of indirectly coupled resonator optical waveguides. The coupling between waveguides and multiple cavities is investigated and the reflection and transmission coefficients are derived.

PACS number(s): 42.79.Gn, 42.25.Bs, 42.60.Da, 42.82.Et

I. INTRODUCTION

It is now well known that a photonic band gap [1–3] exists for certain types of dielectric structure whose dielectric constant varies periodically in space. These types of dielectric structure are generally referred to as photonic crystals. By modifying some unit cells within the photonic crystal, we can create defects may support localized high Q modes [4–6] or propagating waveguide modes [4,7]. If we couple the localized defect modes with waveguides, many interesting phenomena will occur [8–15]. For example, resonant tunneling through the photonic crystal via the localized defect modes has been numerically analyzed [8,9] and experimentally observed [10,11]. Recently, a channel add-drop filter based on coupled waveguide-resonator systems in a photonic crystal was proposed [12–14]. It was shown that, for defect cavities satisfying certain symmetry and degeneracy conditions, optical signals can be completely transferred from one waveguide to another. Waveguide-resonator coupling has also been explored in many other geometries, such as coupled fiber-ring geometry [16], coupled fiber-sphere geometry [17,18], or coupled semiconductor slab waveguide-microring geometry [19–21]. It is intuitively clear that the presence of a resonator should have a profound impact on the reflection and transmission characteristics of the waveguide. For a system composed of a waveguide and a resonator that supports traveling wave modes, it was recently demonstrated that the transmission characteristics depend critically on the balance between waveguide-resonator coupling and cavity loss; thus it was named ''critical coupling'' [22]. In this paper, we use scattering theory to show that for the general system of coupled waveguide-resonator as shown in Fig. 1(a), the reflection and transmission coefficients depend critically on the waveguide-resonator coupling, the symmetry and degeneracy of the resonant modes, cavity loss (gain), and mode resonant frequency.

Besides the much studied waveguide-resonator coupling, multiple optical resonators that are directly coupled together via an evanescent optical field have also been investigated in the literature, such as photonic molecules [23–25], an impurity band in an infinite chain of spheres with negative dielectric constant [26], and coupled resonator optical waveguides (CROW's) [27,28]. All these geometries can be well understood using the tight-binding approximation [29], where the optical mode of the whole system can be regarded as a linear combination of the optical modes within each individual cavity. As a result of the direct coupling between the nearest resonators, many interesting phenomena, such as mode frequency splitting in photonic molecules and waveguiding in CROW's, will occur. If we couple multiple resonators with a waveguide, then as well as direct resonator-resonator coupling the resonators can also be indirectly coupled together by the propagating modes within the waveguide, as shown in Fig. 1(b). We call this type of waveguide an indirect CROW since the cavities are indirectly coupled together. A unique feature of such an indirect CROW is that the tight-binding approximation no longer applies, since any two resonators (not just the neighboring resonators) in Fig. 1(b) can be coupled through the waveguide modes. Based on scattering theory, we propose a matrix formalism to study this type of CROW.

Another natural application of scattering analysis is to find the reflection and transmission coefficients for complicated coupled waveguide-resonator system. In the literature, many different numerical algorithms [8,9,30–33] have been used to find the scattering characteristics of various dielectric

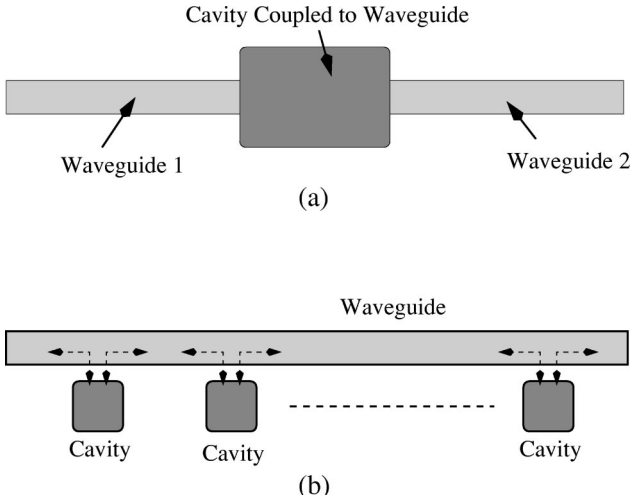

FIG. 1. (a) The general geometry of a waveguide coupled with a cavity. (b) Example of a CROW with indirect coupling.

structures. The benefit of the numerical approach is that it is capable of analyzing dielectric structures of complicated geometries, such as photonic crystals. On the other hand, the numerical calculations are often time consuming and cannot be easily generalized. Since the dielectric structure considered here can be separated into waveguides and localized high Q resonators, its scattering amplitude can be found analytically. In this paper, we use scattering theory to analyze cases where multiple cavities are coupled to a waveguide and give the scattering amplitude of these structures. It is also worth mentioning that coupled mode theory has also been used to treat coupled waveguide-resonator systems, if the resonator supports only one high Q mode [14,34].

The scattering theory formalism of this paper is based on the quantum Lippman-Schwinger equation [35] and resembles the method applied in Ref. [13], where the photonic crystal defect cavity add-drop filter was analyzed. We briefly summarize the scattering theory in Sec. II and discuss some additional important points that were not previously addressed. In Sec. III, we utilize the scattering theory to study two generic cases of coupled waveguide-resonator systems and derive their optical reflection and transmission coefficients. Based on these results, we analyze several simple systems in Sec. IV and discuss in detail the dependence of the optical reflection and transmission on the cavity mode properties and waveguide-resonator coupling. Next, in Sec. V, we propose the concept of an indirect CROW and give an expression for its photonic dispersion relation. In Sec. VI, we give the scattering analysis of more complicated coupled waveguide-resonator systems. We summarize the results in Sec. VII.

II. SCATTERING-THEORY FORMALISM

The Maxwell equation can be rewritten in the form

$$i\frac{\partial}{\partial t}\psi=\mathbf{H}\psi, \tag{2.1a}$$

$$\psi=\begin{bmatrix}\vec{E}\\ \vec{H}\end{bmatrix},\quad \mathbf{H}=\begin{bmatrix}0 & (i/\epsilon)\vec{\nabla}\times\\ (-i/\mu_0)\vec{\nabla}\times & 0\end{bmatrix}. \tag{2.1b}$$

If we introduce the inner product as

$$\langle\psi_2|\psi_1\rangle=\frac{1}{2}\left(\int d^3r\,\epsilon(\vec{r})\vec{E}_2^*\cdot\vec{E}_1+\mu_0\int d^3r\,\vec{H}_2^*\cdot\vec{H}_1\right), \tag{2.2}$$

it is easy to verify that the Hamiltonian $\mathbf{H}$ is a Hermitian operator. For the weakly coupled waveguide-resonator system as shown in Fig. 1(a), the Hamiltonian $\mathbf{H}$ can be separated into a 0th order approximation $\mathbf{H}_0$ where the waveguide modes and the localized high Q modes are independent, and a perturbation term $\mathbf{V}$ that couples them together,

$$\mathbf{H}=\mathbf{H}_0+\mathbf{V}, \tag{2.3a}$$

$$\mathbf{H}_0=\sum_{k_i}\omega_{k_i}|k_i\rangle\langle k_i|+\sum_n\Omega_n|n\rangle\langle n|, \tag{2.3b}$$

$$\mathbf{V}=\sum_{m\neq n}V_{m,n}|m\rangle\langle n|+\sum_{n,k_i}(V_{n,k_i}|n\rangle\langle k_i|+V_{k_i,n}|k_i\rangle\langle n|). \tag{2.3c}$$

In this Hamiltonian we use $|n\rangle$ to represent the nth high Q optical mode with ''bare'' resonant frequency Ω_n, and $|k_i\rangle$ to represent the waveguide mode with wave vector k_i. Here we assume that the waveguide supports only one propagating mode, since multimode waveguides are usually undesirable in optoelectronics applications. Both $|k_i\rangle$ and $|n\rangle$ are normalized to 1 according to Eq. (2.2). We also require $V_{m,n}=V_{n,m}^*$ and $V_{n,k_i}=V_{k_i,n}^*$, since the Hamiltonian is Hermitian. In this Hamiltonian, we ignore the direct coupling between the waveguide modes (i.e., $V_{k_i,k_j}=0$), which will be justified later in this paper. An explicit form for the perturbation term $V_{j,i}$ can be obtained from Eq. (2.1) and Eq. (2.2),

$$V_{j,i}=\langle\psi_j|\mathbf{V}|\psi_i\rangle=\frac{\omega_i}{2}\int d^3r\,[\epsilon_0(\vec{r})]^2\Delta\left[\frac{1}{\epsilon(\vec{r})}\right]\vec{E}_j^*\cdot\vec{E}_i, \tag{2.4}$$

where $\vec{E}_i$ and $\vec{E}_j$ are, respectively, the electric fields associated with modes $|\psi_i\rangle$ and $|\psi_j\rangle$, ω_i is the resonant frequency of mode $|\psi_i\rangle$, $\epsilon_0(\vec{r})$ refers to the dielectric constant of the unperturbed Hamiltonian $\mathbf{H}_0$, and $\Delta[1/\epsilon(\vec{r})]$ is the difference of $1/\epsilon(\vec{r})$ between the full Hamiltonian $\mathbf{H}$ and its 0th order approximation $\mathbf{H}_0$.

Following Ref. [13], we use the waveguide mode $|k_i\rangle$ as the incident optical wave, and assume that the total wave function is given by $|\psi_{total}\rangle$. These two states $|k_i\rangle$ and $|\psi_{total}\rangle$ are related via the scattering matrix $\mathbf{T}$ [35]

$$|\psi_{total}\rangle=|k_i\rangle+\frac{1}{\omega_{k_i}-\mathbf{H}_0+i\epsilon}\mathbf{V}|\psi_{total}\rangle=\mathbf{T}|k_i\rangle, \tag{2.5}$$

where ϵ is a positive infinitesimal number to enforce the outgoing boundary condition. It is easy to verify that the scattering matrix $\mathbf{T}$ can be expressed as

$$\begin{aligned}T_{k_j,k_i}&=\langle k_j|\mathbf{T}|k_i\rangle\\ &=\delta_{k_j,k_i}+\frac{1}{\omega_{k_i}-\omega_{k_j}+i\epsilon}\sum_{m,n}V_{k_j,m}G_{m,n}\\ &\quad\times(\omega_{k_i})V_{n,k_i},\end{aligned} \tag{2.6a}$$

$$T_{n,k_i}=\langle n|\mathbf{T}|k_i\rangle=\sum_m G_{n,m}(\omega_{k_i})V_{m,k_i}, \tag{2.6b}$$

where in Eq. (2.6a) δ_{k_j,k_i} is 1 if $k_i=k_j$ and zero otherwise. The physical meaning of Eq. (2.6a) is clear: The state $|k_i\rangle$ can be scattered into the state $|k_j\rangle$ in two ways, the direct transition as represented by δ_{k_j,k_i}, and the indirect transition through the localized high Q modes $|n\rangle$ as represented by the second term on the right-hand side of Eq. (2.6a). The term $G_{m,n}$ represents the matrix element of the ''renormalized'' Green function $\mathbf{G}$ and is given by $G_{m,n}(\omega)=\langle m|(\omega-\mathbf{H}+i\epsilon)^{-1}|n\rangle$. Its inverse matrix $\mathbf{G}^{-1}$ can be evaluated as

$$(G^{-1})_{m,n}=(\omega-\Omega_n)\delta_{m,n}-\Sigma_{m,n}, \tag{2.7a}$$

$$\Sigma_{m,n}(\omega)=V_{m,n}+\sum_{k_i} V_{m,k_i}\frac{1}{\omega-\omega_{k_i}+i\epsilon}V_{k_i,n}. \tag{2.7b}$$

The derivation of Eqs. (2.6) and (2.7) can be found in Appendix A. Generally, the $\mathbf{\Sigma}$ matrix has some off-diagonal elements, so that finding the renormalized Green function $\mathbf{G}$ can be quite involved. However, in some cases where the high Q resonators have definite symmetry properties, $\mathbf{\Sigma}$ is already diagonalized by the unperturbed states $|n\rangle$. Therefore the renormalized Green function can be simply written as

$$G_{m,n}(\omega)=\frac{1}{\omega-\omega_n+i\Gamma_n}\delta_{m,n}, \tag{2.8}$$

where ω_n is the renormalized frequency of mode $|n\rangle$ and Γ_n is the mode decay rate.

Now we can justify the neglect of the direct waveguide mode interaction V_{k_j,k_i} in the Hamiltonian Eq. (2.3). With such a term, the scattering matrix will have an additional nonresonant contribution $T^{nr}_{k_j,k_i}\sim V_{k_j,k_i}/(\omega_{k_i}-\omega_{k_j}+i\epsilon)$ [see Eq. (2.5)]. Comparing this quantity with the resonant scattering amplitude $T^{r}_{k_j,k_i}$ due to the nth mode, we have

$$\frac{T^{r}_{k_j,k_i}}{T^{nr}_{k_j,k_i}}\sim\frac{V_{k_j,n}G_{n,n}V_{n,k_i}}{V_{k_j,k_i}}, \tag{2.9}$$

where we have used Eq. (2.6a). If the waveguide length is L, V_{k_j,k_i} is of the order of ω_{k_i}/L according to Eq. (2.4), while $V_{k_j,n}V_{n,k_i}$ is of the order of $\omega^2_{k_i}/L$. Substituting Eq. (2.8) into the above equation, it is obvious that the indirect scattering via the nth high Q mode has an enhancement factor of $\omega_{k_i}/(\omega_{k_i}-\omega_n+i\Gamma_n)$. Therefore, if we are interested in the resonant behavior, the direct waveguide mode interaction V_{k_j,k_i} can generally be ignored.

Besides enhanced scattering amplitude, the optical intensity in the resonators is also increased. From Eq. (2.6b) and Eq. (2.8), we find the localized mode amplitude to be

$$T_{n,k_i}=\langle n|\mathbf{T}|k_i\rangle=\frac{V_{n,k_i}}{\omega_{k_i}-\omega_n+i\Gamma_n}, \tag{2.10}$$

which means that the mode amplitude at the resonance is inversely proportional to the mode decay rate.

The mode decay rate Γ_n plays an important role in the problem of waveguide-resonator coupling and can be calculated as follows. Using Eq. (2.7), we find

$$\Sigma_{n,n}(\omega)=\sum_{k_i}|V_{n,k_i}|^2\frac{1}{\omega-\omega_{k_i}+i\epsilon}$$
$$=\frac{L}{2\pi}\int d\omega_{k_i}\frac{1}{v_g}(|V_{n,k_i}|^2+|V_{n,-k_i}|^2)\frac{1}{\omega-\omega_{k_i}+i\epsilon}, \tag{2.11}$$

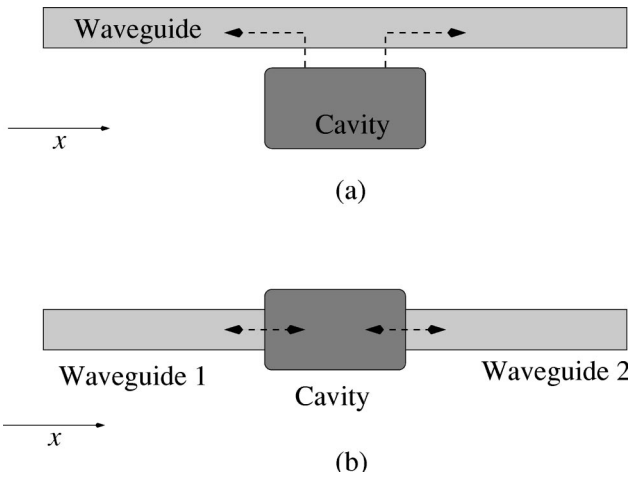

FIG. 2. (a) The side coupling case, where a cavity is side coupled to a waveguide. (b) The resonant coupling case, where two waveguides are coupled by a high Q cavity.

where k_i is the wave vector of the propagating mode, and v_g represents the photon group velocity and is assumed to be positive for any $k_i>0$. Evaluating the integral, we find

$$\mathrm{Im}(\Sigma_{n,n})=-\frac{L}{2v_g}(|V_{n,k_i}|^2+|V_{n,-k_i}|^2). \tag{2.12}$$

If the mode representation $|n\rangle$ is chosen such that only the diagonal elements of $\mathbf{\Sigma}$ are nonzero, the total decay rate of the mode $|n\rangle$ is simply

$$\Gamma_n=\Gamma^0_n+\frac{L}{2v_g}(|V_{n,k_i}|^2+|V_{n,-k_i}|^2), \tag{2.13}$$

where Γ^0_n is the intrinsic cavity decay rate. We should note that in Eq. (2.13) the decay rate is actually independent of the waveguide length L, since $\langle k_i|k_i\rangle=1$ and thus V_{n,k_i} is proportional to $1/\sqrt{L}$.

Once the scattering matrix $\mathbf{T}$ is known, the optical reflection and transmission coefficients can easily be found as follows. If we use $\psi_i(\vec{r}),\psi_r(\vec{r})$, and $\psi_t(\vec{r})$ to represent the incident wave, the reflected wave, and the transmitted wave, respectively, then they can be related to the $\mathbf{T}$ matrix through the following simple relations:

$$\psi_i(\vec{r})+\psi_r(\vec{r})=\langle x\to-\infty|T|k_i\rangle=\sum_{k_j}\langle x\to-\infty|k_j\rangle T_{k_j,k_i}, \tag{2.14a}$$

$$\psi_t(\vec{r})=\langle x\to+\infty|T|k_i\rangle=\sum_{k_j}\langle x\to+\infty|k_j\rangle T_{k_j,k_i}. \tag{2.14b}$$

This method is essentially the same as that in Ref. [13].

III. OPTICAL SCATTERING IN TWO GENERIC COUPLED WAVEGUIDE-RESONATOR SYSTEMS

We study two generic cases of coupled waveguide-resonator systems as illustrated in Fig. 2. The case in Fig. 2(a) is denoted as the ''side coupling'' case, since the reso-

nator is located at the side of an infinite waveguide. For the geometry shown in Fig. 2(b), the two half waveguides are coupled together via resonant tunneling through the center cavity. Consequently we name it the ''resonant coupling'' case. It should be noted that the waveguides and resonators in Fig. 2 can be of any type. In particular, the analysis of this section applies to photonic crystal waveguides and defect cavities. Therefore, we assume that the waveguides possess a one-dimensional discrete translational symmetry. Waveguides with continuous translational symmetry, such as slab waveguides or optical fibers, can be regarded as a special case.

First let us consider the side coupling case. We assume that the waveguide mode $|k_i\rangle$ has the following general form (using the Bloch theorem):

$$\phi_{k_i}(\vec{r}) = \frac{1}{\sqrt{N}} u_{k_i}(\vec{r}) e^{ik_i x}, \tag{3.1a}$$

$$u_{k_i}(\vec{r}) = u_{k_i}(\vec{r} + R\hat{e}_x), \tag{3.1b}$$

where N is the total number of unit cells in the waveguide and $u_{k_i}(\vec{r})$ is normalized to 1 within a unit cell. R is the length of a unit cell.

We assume that the incoming wave is the waveguide mode $|k_i\rangle$. Therefore, the incident wave $\psi_i(\vec{r})$ in Eq. (2.14) is simply $\phi_{k_i}(\vec{r})$ and the transmitted wave $\psi_t(\vec{r})$ at $x \to +\infty$ is

$$\psi_t(\vec{r}) = \phi_{k_i}(\vec{r}) + \sum_n \frac{V_{n,k_i}}{\omega_{k_i} - \omega_n + i\Gamma_n} \frac{L}{2\pi\sqrt{N}} \times \int dk_j u_{k_j} e^{ik_j x} \frac{V_{k_j,n}}{-v_g(k_j - k_i) + i\epsilon}, \tag{3.2}$$

where Eq. (2.6a), Eq. (2.8), and Eq. (2.14) are used, and we transform the summation over k_j into an integral. Evaluating the integral, we find the transmitted wave to be

$$\psi_t(\vec{r}) = \frac{1}{\sqrt{N}} u_{k_i}(\vec{r}) e^{ik_i x} \left[1 - i \sum_n \frac{1}{\omega_{k_i} - \omega_n + i\Gamma_n} \frac{L|V_{k_i,n}|^2}{v_g} \right], \tag{3.3a}$$

$$\Gamma_n = \Gamma_n^0 + \frac{L(|V_{k_i,n}|^2 + |V_{-k_i,n}|^2)}{2v_g}. \tag{3.3b}$$

In a similar way, we use Eq. (2.14) and find the optical wave at $x \to -\infty$ to be

$$\psi_i(\vec{r}) + \psi_r(\vec{r}) = \phi_{k_i}(\vec{r}) + \sum_n \frac{V_{n,k_i}}{\omega_{k_i} - \omega_n + i\Gamma_n} \sum_{k_j} \phi_{k_j}(\vec{r}) \times \frac{V_{k_j,n}}{\omega_{k_i} - \omega_{k_j} + i\epsilon}. \tag{3.4}$$

We transform the summation over k_j into an integral and find $\psi_r(\vec{r})$ to be

$$\psi_r(\vec{r}) = -i \sum_n \frac{1}{\omega_{k_i} - \omega_n + i\Gamma_n} \frac{L V_{-k_i,n} V_{n,k_i}}{v_g} \times \left[\frac{1}{\sqrt{N}} u_{-k_i}(\vec{r}) e^{-ik_i x} \right]. \tag{3.5}$$

If we use r and t to denote the amplitude reflection and transmission coefficient, respectively the above results can be summarized as

$$r = -i \sum_n \frac{1}{\omega_{k_i} - \omega_n + i\Gamma_n} \frac{L V_{-k_i,n} V_{n,k_i}}{v_g}, \tag{3.6a}$$

$$t = 1 - i \sum_n \frac{1}{\omega_{k_i} - \omega_n + i\Gamma_n} \frac{L|V_{k_i,n}|^2}{v_g}, \tag{3.6b}$$

$$\Gamma_n = \Gamma_n^0 + \frac{L(|V_{k_i,n}|^2 + |V_{-k_i,n}|^2)}{2v_g}. \tag{3.6c}$$

The side coupling geometry can actually be regarded as part of the photonic crystal add-drop filter considered in Ref. [12–14]. The above results are also similar to those in Ref. [13]. However, we also point out a subtle but important difference: we consider the possibility of gain or loss in the cavity, which is represented by Γ_n^0 in Eq. (3.6). A more detailed discussion will be given in the next section.

Next we study the case of resonant coupling as shown in Fig. 2(b), which to the best of our knowledge has not been analyzed before using the scattering-theory formalism. Here for notational convenience we assume that both waveguides are along the x direction, even though the results do not depend on this assumption. In reality, the two waveguides can have an arbitrary bending angle, as long as the direct interaction between them can be ignored.

We assume that both waveguides consist of N unit cells, and the normalized waveguide modes in waveguide 1 and waveguide 2 are uncoupled and can be expressed, respectively, as

$$\langle \vec{r}|k_i\rangle = \frac{1}{\sqrt{2N}} [u_{k_i}(\vec{r}) e^{ik_i x} + u_{k_i}^*(\vec{r}) e^{-ik_i x}] \quad \text{in waveguide 1;} \tag{3.7a}$$

$$\langle \vec{r}|q_j\rangle = \frac{1}{\sqrt{2N}} [v_{q_j}(\vec{r}) e^{iq_j x} + v_{q_j}^*(\vec{r}) e^{-iq_j x}] \quad \text{in waveguide 2.} \tag{3.7b}$$

We use $|k_i\rangle$ and $|q_j\rangle$ to represent modes in waveguide 1 and waveguide 2, with k_i and q_j referring to their wave vectors. As before, both $u_{k_i}(\vec{r})$ and $v_{q_j}(\vec{r})$ are normalized within a unit cell. We assume that the unit cell length in waveguide 1 is R_1 and the total waveguide length is $L_1 = NR_1$. For waveguide 2, the unit cell length is R_2 and the total length is $L_2 = NR_2$.

According to Eq. (2.14), the optical wave at $x \to -\infty$ (in waveguide 1) consists of the incident wave $\psi_i(\vec{r})$ and the reflected wave $\psi_r(\vec{r})$:

$$\psi_i(\vec{r})+\psi_r(\vec{r})=\int dk_j \frac{L_1}{\pi\sqrt{2N}}[u_{k_j}e^{ik_jx}+\text{c.c.}] \times\left[\delta_{k_j,k_i}+\frac{1}{\omega_{k_i}-\omega_{k_j}+i\epsilon}\sum_n \frac{V_{k_j,n}V_{n,k_i}}{\omega_{k_i}-\omega_n+i\Gamma_n}\right]. \tag{3.8}$$

Evaluating the integral, we find

$$\psi_i(\vec{r})=\frac{1}{\sqrt{2N}}u_{k_i}(\vec{r})e^{ik_ix}, \tag{3.9a}$$

$$\psi_r(\vec{r})=\frac{1}{\sqrt{2N}}u^*_{k_i}(\vec{r})e^{-ik_ix}\left[1-i\sum_n \frac{|V_{k_i,n}|^2}{\omega_{k_i}-\omega_n+i\Gamma_n}\frac{2L_1}{v_g^1}\right], \tag{3.9b}$$

where v_g^1 is the photon group velocity in waveguide 1 and is assumed to be positive. The transmitted wave $\psi_t(\vec{r})$ at $x\to+\infty$ (in waveguide 2) can be found similarly, as

$$\begin{aligned}\psi_t(\vec{r})&=\frac{L_2}{\pi\sqrt{2N}}\int dq_j(v_{q_j}e^{iq_jx}+\text{c.c.}) \times\frac{1}{\omega_{k_i}-\omega_{q_j}+i\epsilon}\sum_n\frac{V_{q_j,n}V_{n,k_i}}{\omega_{k_i}-\omega_n+i\Gamma_n}\\ &=\frac{1}{\sqrt{2N}}v_{q_j}(\vec{r})e^{iq_jx} \times\left[-2i\sum_n\frac{1}{\omega_{k_i}-\omega_n+i\Gamma_n}\frac{L_2V_{q_j,n}V_{n,k_i}}{v_g^2}\right],\end{aligned} \tag{3.10}$$

where q_j is the wave vector of the propagating mode in waveguide 2 and is determined by the condition $\omega_{q_j}=\omega_{k_i}$, and v_g^2 is the corresponding photon group velocity and is assumed to be positive.

Since the photons in the high Q cavity can independently decay into both waveguide 1 and waveguide 2, the decay rate of the nth mode Γ_n will simply be the sum of the two processes. Collecting the results, for the resonant coupling case, we have

$$\psi_i(\vec{r})=\frac{1}{\sqrt{2N}}u_{k_i}(\vec{r})e^{ik_ix}, \tag{3.11a}$$

$$\psi_r(\vec{r})=\frac{1}{\sqrt{2N}}u^*_{k_i}(\vec{r})e^{-ik_ix} \times\left[1-i\sum_n\frac{1}{\omega_{k_i}-\omega_n+i\Gamma_n}\frac{2L_1|V_{k_i,n}|^2}{v_g^1}\right], \tag{3.11b}$$

$$\psi_t(\vec{r})=\frac{1}{\sqrt{2N}}v_{q_j}(\vec{r})e^{iq_jx} \times\left[-i\sum_n\frac{1}{\omega_{k_i}-\omega_n+i\Gamma_n}\frac{2L_2V_{q_j,n}V_{n,k_i}}{v_g^2}\right], \tag{3.11c}$$

$$\Gamma_n=\Gamma_n^0+\frac{L_1|V_{n,k_i}|^2}{v_g^1}+\frac{L_2|V_{n,q_j}|^2}{v_g^2}. \tag{3.11d}$$

The cavity mode decay rate Γ_n in Eq. (3.11d) is different from Eq. (2.13), because we assume the waveguide supports traveling waves in deriving Eq. (2.13), yet the waveguide modes we use in the resonant coupling case are essentially standing waves [see Eq. (3.7)]. It is interesting to compare the above results, Eq. (3.11), with Eq. (3.6), and observe that the reflection and transmission in the resonant coupling case correspond, respectively, to the transmission and reflection in the side coupling geometries.

The Bloch wave functions u_{k_i} or v_{q_j} in Eq. (3.7) are normalized to 1 within a unit cell. Thus the power flux P in the waveguide satisfies the relation

$$P\propto|A|^2\frac{v_g}{R}, \tag{3.12}$$

where R is the size of a unit cell, v_g is the photon group velocity, and A is the amplitude of the optical wave. As an example, $A=\exp(ik_ix)/\sqrt{2N}$ for the incident wave $\psi_i(\vec{r})$ in Eq. (3.11a). Combining Eq. (3.11) and Eq. (3.12), we find the power reflection coefficient R and transmission coefficient T to be

$$R=\left|1-i\sum_n\frac{1}{\omega_{k_i}-\omega_n+i\Gamma_n}\frac{2L_1|V_{k_i,n}|^2}{v_g^1}\right|^2, \tag{3.13a}$$

$$T=\left|\sum_n\frac{1}{\omega_{k_i}-\omega_n+i\Gamma_n}\frac{2L_2V_{q_j,n}V_{n,k_i}}{v_g^2}\right|^2\frac{v_g^2R_1}{v_g^1R_2}. \tag{3.13b}$$

IV. CRITICAL COUPLING IN COUPLED WAVEGUIDE-RESONATOR SYSTEMS

The simplest case of side coupling is a single mode resonator coupled with a single mode waveguide, as shown in Fig. 3(a). It is worth mentioning that a specific example of this side coupling geometry has been investigated in Ref. [34], where the single mode resonator is the quarter wave shifted distributed feedback resonator. In our case, the cavity decay rate Γ^c due to the presence of waveguide is given by Eq. (2.13),

$$\Gamma^c=\Gamma^c_-+\Gamma^c_+=\frac{L}{2v_g}|V_{n,-k}|^2+\frac{L}{2v_g}|V_{n,k}|^2, \tag{4.1}$$

where we use $\Gamma^c_-=(L/2v_g)|V_{n,-k}|^2$ and $\Gamma^c_+=(L/2v_g)|V_{n,k}|^2$ to represent the decay in the $-\hat{x}$ and $+\hat{x}$

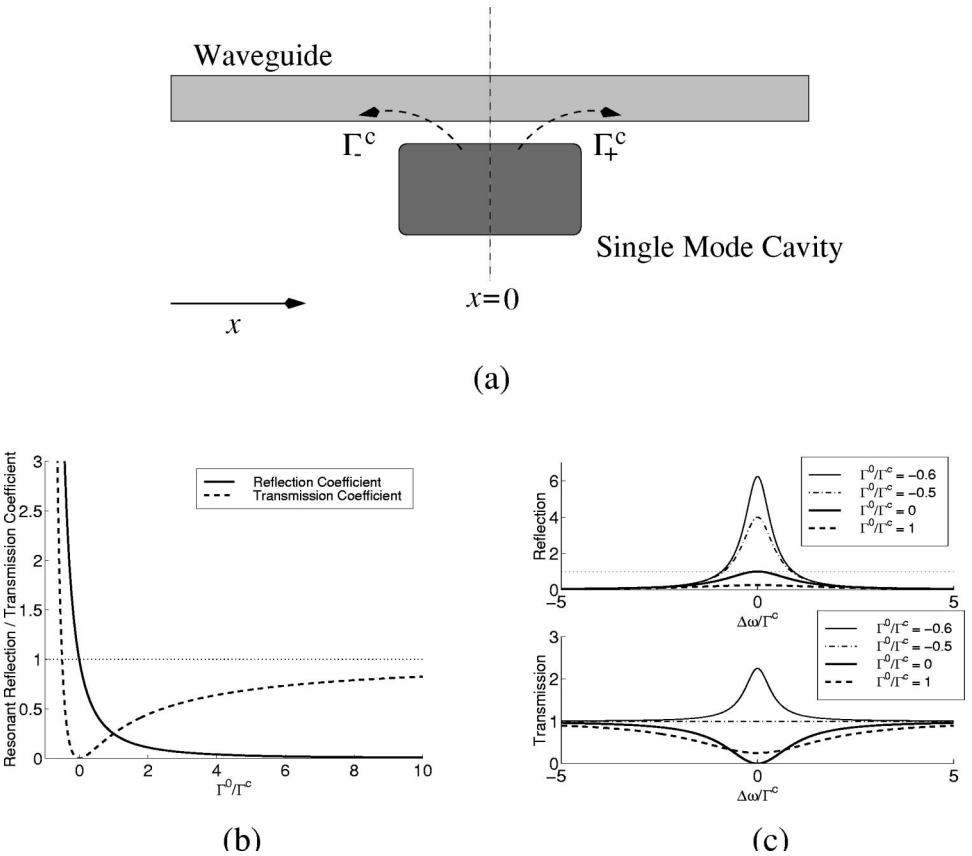

FIG. 3. (a) Sketch of a single mode resonator side coupled to a single mode waveguide. Γ_-^c and Γ_+^c are, respectively, the cavity decay rate in the $-\hat{x}$ and $+\hat{x}$ directions. For a resonator with mirror reflection symmetry with respect to the $x=0$ plane, $\Gamma_-^c=\Gamma_+^c$. (b) The resonant $(\Delta\omega=0)$ reflection and transmission coefficients for the waveguide side coupled to a single mode resonator. Γ^0 represents the intrinsic cavity loss (gain), and Γ^c is the decay rate of the cavity mode into the waveguide. (c) Reflection and transmission spectra for four different values of Γ^0/Γ^c.

directions, respectively. A further simplification is possible if the cavity possesses a mirror reflection symmetry with respect to the $x=0$ plane, which gives $\Gamma_-^c=\Gamma_+^c=\Gamma_c/2$. From Eq. (3.6), we find the power reflection coefficient R and transmission coefficient T to be

$$R=|r|^2=\frac{(\Gamma^c)^2}{\Delta\omega^2+(\Gamma^0+\Gamma^c)^2}, \tag{4.2a}$$

$$T=|t|^2=\frac{\Delta\omega^2+(\Gamma^0)^2}{\Delta\omega^2+(\Gamma^0+\Gamma^c)^2}, \tag{4.2b}$$

where Γ^0 represents the intrinsic loss (gain) of the resonator, and $\Delta\omega$ is $\omega-\Omega$, with ω being the frequency of the incident light and Ω being the resonant mode frequency.

In Fig. 3(b), we show the resonant $(\Delta\omega=0)$ reflection coefficient R and transmission coefficient T as functions of Γ^0/Γ^c. Notice that at $\Gamma^0/\Gamma^c=0$ the resonant transmission coefficient T becomes zero and the reflection coefficient R is 1. On the other hand, when the intrinsic cavity loss is much larger than the cavity-waveguide coupling, i.e., $\Gamma^0/\Gamma^c\gg1$, the transmission coefficient approaches 1 and the reflection coefficient almost vanishes. If we introduce gain into the cavity and the lasing condition is approached, i.e., $\Gamma^0/\Gamma^c\rightarrow-1$, both R and T become very large. In Fig. 3(c), we plot the transmission and reflection spectra using different values of Γ^0/Γ^c, which clearly shows the critical dependence of the reflection and transmission characteristics on both $\Delta\omega$ and Γ^0/Γ^c. Of particular interest is the case of $\Gamma^0/\Gamma^c=-0.5$, which gives a flat transmission coefficient equal to 1. An obvious application of this critical dependence, similar to the phenomenon of critical coupling observed in Ref. [22], is the possibility of controlling optical transmission and reflection by tuning $\Delta\omega$, Γ^0, or Γ^c.

In reality, it is difficult to fabricate a dielectric structure with perfect mirror reflection symmetry and there will always be some small difference between Γ_+^c and Γ_-^c. With symmetry broken, the reflection coefficient R and transmission coefficient T are

$$R=|r|^2=\frac{4\Gamma_-^c\Gamma_+^c}{\Delta\omega^2+(\Gamma^0+\Gamma_-^c+\Gamma_+^c)^2}, \tag{4.3a}$$

$$T=|t|^2=\frac{\Delta\omega^2+(\Gamma^0+\Gamma_-^c-\Gamma_+^c)^2}{\Delta\omega^2+(\Gamma^0+\Gamma_-^c+\Gamma_+^c)^2}. \tag{4.3b}$$

These results show that the general reflection and transmission features of the system are not significantly changed. We can still achieve zero resonant $(\Delta\omega=0)$ transmission by tuning $\Gamma^0=\Gamma_+^c-\Gamma_-^c$. Unity transmission can also by achieved by choosing $\Gamma^0=-\Gamma_-^c$.

In the next case, we consider a side coupled cavity that supports two degenerate modes with frequency Ω. We rewrite Eq. (3.6) as

$$r=-i\sum_{n=1}^{2}\frac{1}{\Delta\omega+i\Gamma_n}\frac{L}{v_g}V_{-k,n}V_{n,k}, \tag{4.4a}$$

$$t=1-i\sum_{n=1}^{2}\frac{1}{\Delta\omega+i\Gamma_n}\frac{L}{v_g}|V_{k,n}|^2, \tag{4.4b}$$

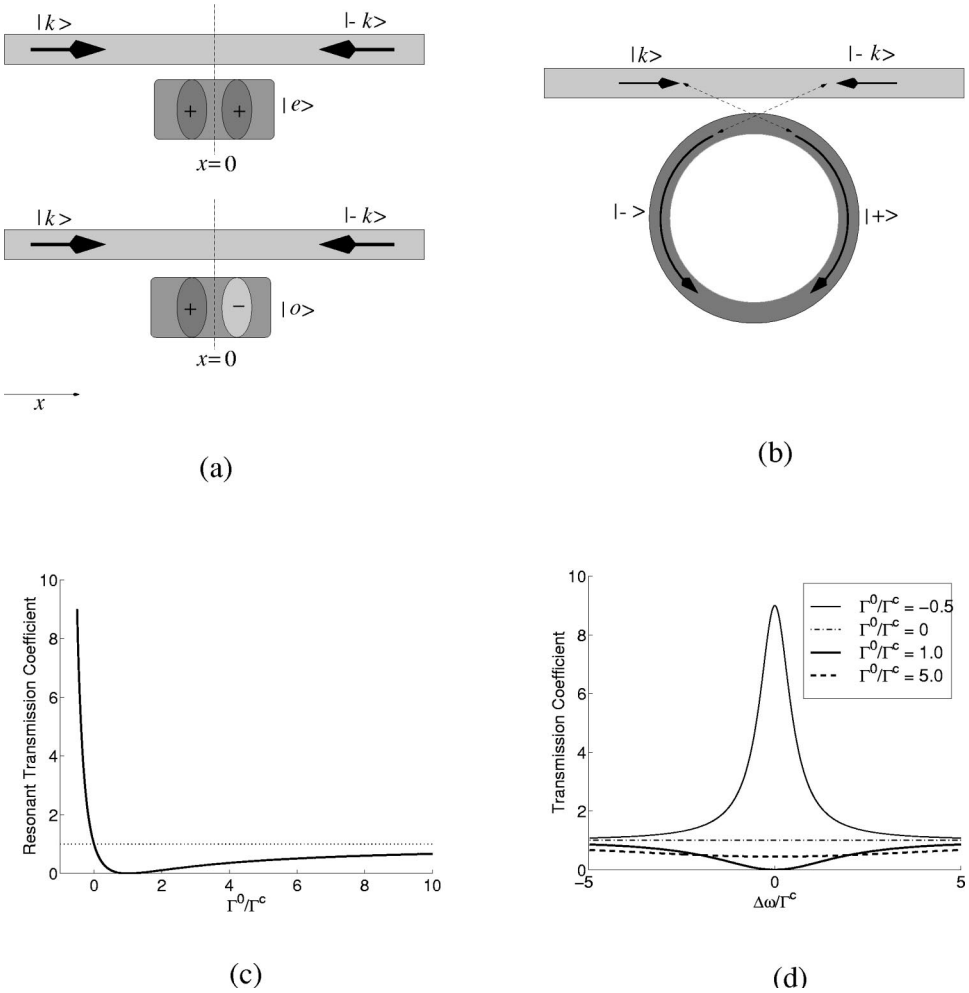

FIG. 4. (a) Sketch of a waveguide side coupled with a cavity supporting two degenerate modes. The cavity possesses a mirror reflection symmetry with respect to the $x=0$ plane and the doubly degenerate modes have opposite parity under mirror reflection. The even mode is $|e\rangle$ and the odd mode is $|o\rangle$. (b) The side coupling geometry where two traveling waves are supported in the cavity. The two modes travel in opposite directions and are degenerate due to the time reversal symmetry. The mode traveling in the clockwise direction is $|+\rangle$ and the mode traveling in the counterclockwise direction is $|-\rangle$. (c) The resonant transmission coefficient as a function of Γ^0/Γ^c. (d) The transmission spectrum for different values of Γ^0/Γ^c.

$$\Gamma_n=\Gamma_n^0+\Gamma_n^c=\Gamma_n^0+\frac{L}{2v_g}|V_{k,n}|^2+\frac{L}{2v_g}|V_{-k,n}|^2, \tag{4.4c}$$

where we use the convention of $\Delta\omega=\omega-\Omega$.

For this doubly degenerate side coupling geometry, two simple cases are of special interest. The first example is when the resonator possesses a mirror reflection symmetry with respect to the $x=0$ plane and the two degenerate modes have opposite parity, as shown in Fig. 4(a). Assuming the even mode is $|e\rangle$ and the odd mode is $|o\rangle$, Eq. (2.4) gives

$$V_{k,e}=V_{-k,e}, V_{k,o}=-V_{-k,o}, \tag{4.5}$$

where $V_{k,e}$ represents the coupling between the incident wave $|k\rangle$ and the even cavity mode $|e\rangle$, and $V_{k,o}$ represents the coupling between $|k\rangle$ and the odd cavity mode $|o\rangle$. We follow Refs. [12,13] and assume that the waveguide mode $|k\rangle$ couples equally strong with the even mode and the odd mode, i.e.,

$$|V_{k,e}|=|V_{k,o}|. \tag{4.6}$$

Consequently, from Eq. (4.4) we obtain

$$R=0, \quad T=\frac{\Delta\omega^2+(\Gamma^0-\Gamma^c)^2}{\Delta\omega^2+(\Gamma^0+\Gamma^c)^2}, \tag{4.7}$$

where Γ^c is $\Gamma^c=L|V_{k,e}|^2/v_g$. We notice the remarkable result that the reflection coefficient R remains 0 for all frequencies. This is a direct consequence of the destructive interference between the reflected waves due to the two degenerate cavity modes, as was pointed out in Ref. [12]. In fact, this side coupling geometry can be regarded as half of the photonic crystal add-drop filters studied in Refs. [12–14]. Here the coupling to the second waveguide is represented by the ''intrinsic'' cavity decay rate Γ^0.

In addition to the condition of frequency degeneracy and equal mode decay rate, Eq. (4.6) must also be strictly satisfied to eliminate reflection. It is very difficult to simultaneously realize these requirements during the fabrication processes. In practice, it is easier to fabricate semiconductor ring or disk resonators [19–21] and dielectric microspheres [17,18], which support two counterpropagating modes, as shown in Fig. 4(b). In the following analysis, we show that the reflection and transmission coefficients of a waveguide coupled to this type of resonator are also described by Eq. (4.7).

If the waveguide mode and the traveling wave mode in the resonator are phase matched, it is safe to assume that the waveguide mode can induce a traveling wave circulating in only one direction. As shown in Fig. 4(b), we denote the clockwise circulating mode as $|+\rangle$ and the counterclockwise mode as $|-\rangle$. Using these notations, the condition for phase-matched coupling is $V_{k,-}=0$ and $V_{-k,+}=0$. Furthermore,

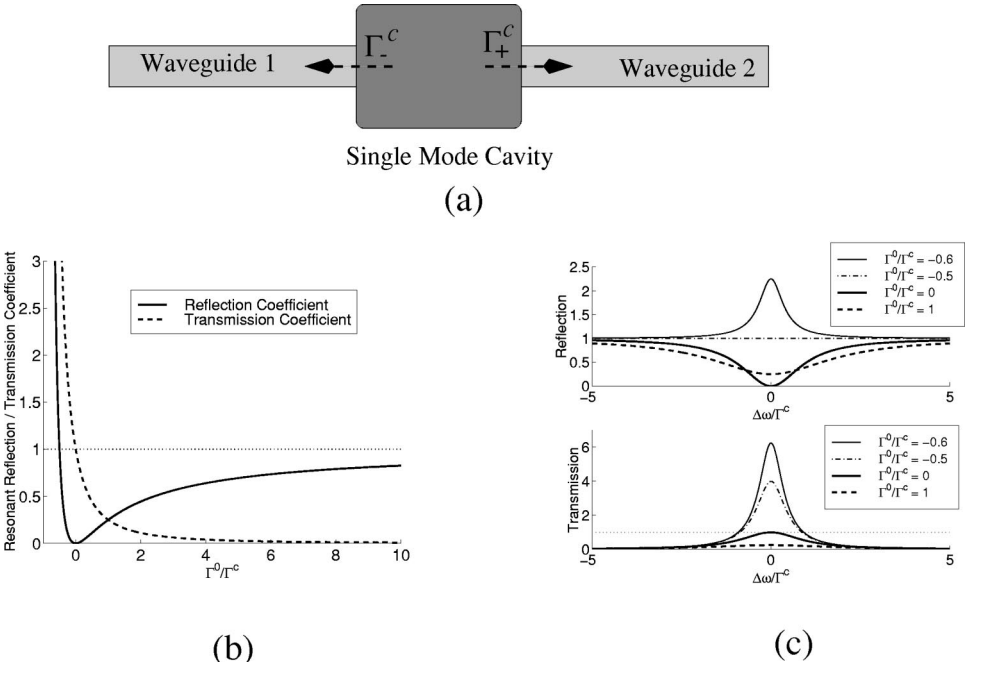

FIG. 5. (a) A sketch of two waveguides of the same type coupled together via a high Q resonator supporting a single mode, which is the simplest case of resonant coupling. (b) The resonant reflection and transmission coefficients of the coupled waveguide-resonator system shown in (a). (c) The reflection and transmission spectra of the coupled waveguide-resonant system with different parameters of Γ^0/Γ^c.

using Eq. (2.4) and the time reversal symmetry, we find $V_{k,+}=V^*_{-k,-}$. With these conditions, from Eq. (4.4) we have

$$R=|r|^2=0, \tag{4.8a}$$

$$T=|t|^2=\frac{\Delta\omega^2+(\Gamma^0-\Gamma^c)^2}{\Delta\omega^2+(\Gamma^0+\Gamma^c)^2}, \tag{4.8b}$$

$$\Gamma^c=\frac{L}{2v_g}|V_{k,+}|^2=\frac{L}{2v_g}|V_{-k,-}|^2. \tag{4.8c}$$

The above result is the same as Eq. (4.7).

In Fig. 4(c), the resonant $(\Delta\omega=0)$ transmission coefficient was plotted as a function of Γ^0/Γ^c. Notice that at $\Gamma^0/\Gamma^c=1$ T is always equal to zero. This phenomenon is the principle behind many add-drop filters studied in the literature [12–14,19–21], and was named critical coupling in Ref. [22]. The above result for T also applies for the case where gain is introduced, i.e., $\Gamma^0<0$. The transmission spectrum is shown in Fig. 4(d) for different values of Γ^0/Γ^c. We notice that when the lasing threshold is approached $(\Gamma^0/\Gamma^c\rightarrow-1)$ the optical wave is amplified and the resonance width is narrowed.

For the case of resonant coupling, we limit ourselves to the simplest case, which is composed of two waveguides coupled via a single mode high Q resonator, as shown in Fig. 5. As a further simplification, we assume that the two waveguides are the same type and have the same unit cell length R and total length L. Thus Eq. (3.13) becomes

$$R=\frac{(\Delta\omega)^2+(\Gamma^0+\Gamma^c_+-\Gamma^c_-)^2}{(\Delta\omega)^2+(\Gamma^0+\Gamma^c_++\Gamma^c_-)^2}, \tag{4.9a}$$

$$T=\frac{4\Gamma^c_-\Gamma^c_+}{(\Delta\omega)^2+(\Gamma^0+\Gamma^c_++\Gamma^c_-)^2}, \tag{4.9b}$$

$$\Gamma^c_-=\frac{L}{v_g}|V_{n,k_i}|^2, \quad \Gamma^c_+=\frac{L}{v_g}|V_{n,q_j}|^2, \tag{4.9c}$$

where as before we use Γ^0 to represent the intrinsic cavity loss or gain, Γ^c_- represents the cavity decay rate into waveguide 1, and Γ^c_+ represents the cavity decay rate into waveguide 2. From the above equations, we find that at resonance $(\Delta\omega=0)$ it is necessary to satisfy the condition of $\Gamma^0=0$ and $\Gamma^c_-=\Gamma^c_+$ to realize $R=0$ and $T=1$ (i.e., photon resonant tunneling).

To reduce the number of parameters in our analysis, we assume $\Gamma^c_-=\Gamma^c_+$, which allows us to use a single parameter $\Gamma^c=2\Gamma^c_-$ and simplify Eq. (4.9) as

$$R=\frac{(\Delta\omega)^2+(\Gamma^0)^2}{(\Delta\omega)^2+(\Gamma^0+\Gamma^c)^2}, \tag{4.10a}$$

$$T=\frac{(\Gamma^c)^2}{(\Delta\omega)^2+(\Gamma^0+\Gamma^c)^2}. \tag{4.10b}$$

It is interesting to notice that the above result is very similar to Eq. (4.2), which gives the reflection and transmission coefficients for a waveguide side-coupled with a single mode waveguide. The only difference between the two cases is that the reflection coefficient in Eq. (4.2) corresponds to the transmission coefficient in Eq. (4.10), and the transmission coefficient in Eq. (4.2) corresponds to the reflection coefficient in Eq. (4.10).

In Fig. 5(b), we show the resonant reflection and transmission coefficients as functions of Γ^0/Γ^c. In Fig. 5(c), we plot the reflection and transmission spectra using various parameters of Γ^0/Γ^c. As expected, we find that Figs. 5(b) and 5(c) are the same as Figs. 3(b) and 3(c), if we identify the transmission and reflection in Fig. 5 with the reflection and transmission, respectively, in Fig. 3.

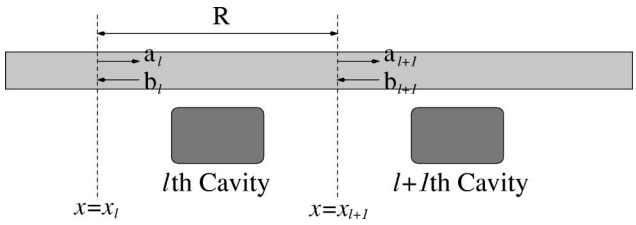

FIG. 6. An example of an indirect CROW, which consists of a waveguide side coupled to an array of high Q resonators.

V. DISPERSION RELATION OF INDIRECT CROW

In the literature, most of the studies on systems of coupled resonators utilized the tight-binding approximation [23–28]. However, for the structure shown in Fig. 6, where a waveguide is side coupled to an array of high Q resonators, the tight-binding approximation no longer applies. It is obvious in Fig. 6 that any two resonators in this type of CROW can be coupled to each other via the propagating modes in the waveguide. We shall name this type of CROW an indirect CROW, since the resonators are indirectly coupled together via the propagating modes in the waveguide. In this section, we develop a matrix formalism to analyze the indirect CROW's.

To simplify our analysis, we limit ourselves to CROW's with large intercavity distance R, which enables us to ignore the direct coupling between the resonators. For the structure shown in Fig. 6, we write the optical wave to the immediate left of the lth unit cell as

$$\begin{aligned}\psi(\vec{r})|_{x=x_l} &= A_l u_k(\vec{r}) + B_l u_k^*(\vec{r}) \\ &= a_l e^{ikx_l} u_k(\vec{r}) + b_l e^{-ikx_l} u_k^*(\vec{r}),\end{aligned} \tag{5.1}$$

where $u_k(\vec{r})$ is defined in Eq. (3.1). We now introduce a matrix formalism, in which a matrix $\mathbf{M}$ is used to relate the optical wave to the left and the optical wave to the right of the lth unit cell,

$$\begin{bmatrix} a_{l+1} \\ b_{l+1} \end{bmatrix} = \mathbf{M} \begin{bmatrix} a_l \\ b_l \end{bmatrix}. \tag{5.2}$$

We notice that this approach is similar to the transfer matrix method that was widely used to describe one-dimensional multilayer structures [36]. Using Eq. (3.3a), Eq. (3.5), Eq. (3.6), and applying time reversal symmetry, we have the following relations for the matrix M:

$$\begin{bmatrix} t \\ 0 \end{bmatrix} = \mathbf{M} \begin{bmatrix} 1 \\ r \end{bmatrix}, \quad \begin{bmatrix} 0 \\ t^* \end{bmatrix} = \mathbf{M} \begin{bmatrix} r^* \\ 1 \end{bmatrix}. \tag{5.3}$$

From these two equations, the matrix M is determined to be

$$\mathbf{M} = \begin{bmatrix} \frac{1}{t^*} & -\frac{r^*}{t^*} \\ -\frac{r}{t} & \frac{1}{t} \end{bmatrix}. \tag{5.4}$$

Combining Eq. (5.1), Eq. (5.2), and Eq. (5.4), we find

$$\begin{bmatrix} A_{l+1} \\ B_{l+1} \end{bmatrix} = \begin{bmatrix} \frac{1}{t^*} e^{ikR} & -\frac{r^*}{t^*} e^{ik(x_l + x_{l+1})} \\ -\frac{r}{t} e^{ik(x_l + x_{l+1})} & \frac{1}{t} e^{-ikR} \end{bmatrix} \begin{bmatrix} A_l \\ B_l \end{bmatrix}. \tag{5.5}$$

The eigenvalue equation for the matrix in the above equation is simply

$$\lambda^2 - \lambda \left(\frac{1}{t} e^{-ikR} + \frac{1}{t^*} e^{ikR} \right) + 1 = 0. \tag{5.6}$$

According to the Bloch theorem and the definition of A_l and B_l in Eq. (5.1), for any propagating wave inside a spatially periodic structure, the eigenvalue λ should be of the form $\exp(\pm i\beta R)$, with β being the Bloch wave vector. Consequently, from Eq. (5.6), we find

$$2\cos(\beta R) = \frac{1}{t} e^{-ikR} + \frac{1}{t^*} e^{ikR}. \tag{5.7}$$

We consider a simple case of a CROW, where the resonator possesses mirror reflection symmetry and supports only a single mode. Under this assumption, the reflection coefficient t is given by Eq. (3.6),

$$t = \frac{\Delta\omega}{\Delta\omega + i\Gamma^c}, \tag{5.8}$$

where we assume the cavity has no loss or gain, i.e., $\Gamma^0 = 0$. The term is defined as $\Gamma^c = L|V_{k,n}|^2/v_g$ and represents the coupling between the cavity and the waveguide. Using Eq. (5.7) and Eq. (5.8), we obtain the dispersion relation for this indirect CROW,

$$\cos(\beta R) = \cos(kR) + \frac{\Gamma^c}{\Delta\omega} \sin(kR). \tag{5.9}$$

Notice that k represents the wave vector of the pure waveguide, and β represents the wave vector of the compound system.

If the quantity $kR \neq n\pi$, a direct consequence of Eq. (5.9) is that no propagating mode exists at the renormalized resonance frequency $\omega = \Omega$. In fact, under the condition of $\sin(kR)$ not close to zero, for any $\Delta\omega$ within the range of Γ^c, the term $\Gamma^c/\Delta\omega$ will be larger than 1. According to Eq. (5.9), this means the formation of a band gap of the order of Γ^c that contains the renormalized resonator frequency Ω. If an unperturbed waveguide band traverses the renormalized resonance frequency at k_0, it is necessary that this waveguide

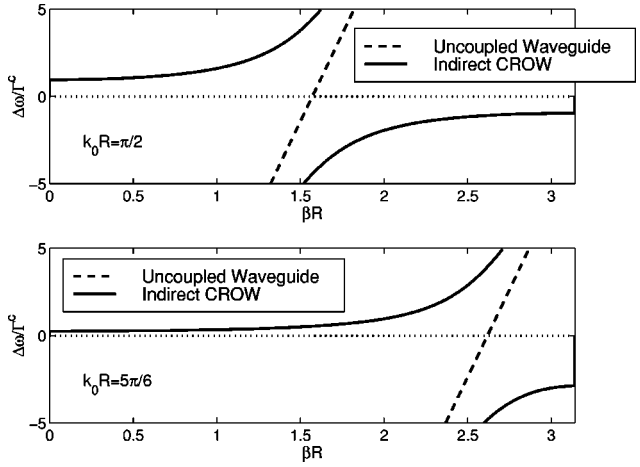

FIG. 7. The uncoupled waveguide band and the photonic band of the indirect CROW calculated from Eq. (5.11). In (a) $k_0R=\pi/2$ and in (b) $k_0R=5\pi/6$. We choose the parameter $R\Gamma^c/v_g=0.05$. The justification for this value is given in the text.

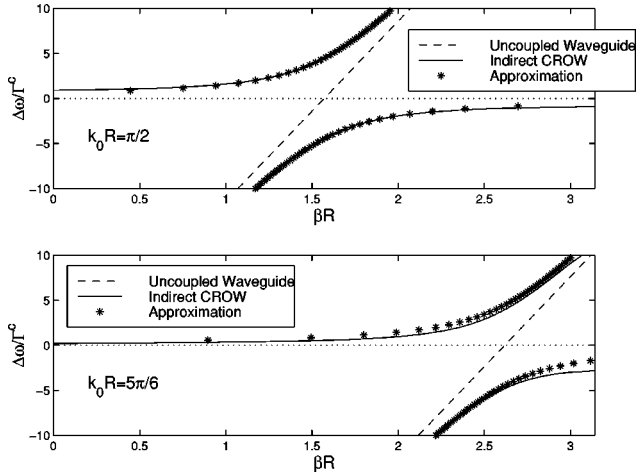

FIG. 8. Dispersion relations of the indirect CROW bands. The solid lines are the exact solutions of Eq. (5.11) with $R\Gamma^c/v_g=0.05$. The dashed line represents the uncoupled waveguide band and the stars are the approximate solutions given by Eq. (5.12). In (a), we use $k_0R=\pi/2$ and in (b) $k_0R=5\pi/6$.

band is split and a band gap is formed due to its coupling to the CROW structure. We assume a linear dispersion relation for the unperturbed waveguide mode,

$$k=k_0+\frac{1}{v_g}\Delta\omega, \tag{5.10}$$

where $\Delta\omega=\omega-\Omega$. This assumption simplifies Eq. (5.9) as

$$\cos(\beta R)=\cos\left(k_0R+\frac{\Delta\omega}{\Gamma^c}\frac{R\Gamma^c}{v_g}\right)+\frac{\Gamma^c}{\Delta\omega}\sin\left(k_0R+\frac{\Delta\omega}{\Gamma^c}\frac{R\Gamma^c}{v_g}\right). \tag{5.11}$$

From this expression, it is obvious that the photonic band structure of the compound waveguide depends critically on k_0R, Γ^c, and R. For many photonic crystals, the mid-gap frequency is typically of the value $\omega a/2\pi c=0.3$, where a is the photonic lattice spacing and c is the light speed in free space [3]. If we consider a compound waveguide formed by a photonic crystal waveguide and defect cavities, we can choose $R=5a, v_g=0.3c$, and the cavity Q (consequently ω/Γ^c) between 100 and 1000. From these estimates, we find that the parameter $R\Gamma^c/v_g$ is of the order of 0.05. In Fig. 7, we use $R\Gamma^c/v_g=0.05$ and plot the indirect CROW band as calculated from Eq. (5.11). It is clearly demonstrated in Fig. 7 that the photonic band of the indirect CROW splits at $\Delta\omega=0$ and its resonant band structure depends critically on the value of k_0R.

On the other hand, if the propagating mode frequency is far away from resonance, Eq. (5.9) can be solved asymptotically. For $\Delta\omega\gg\Gamma^c,\beta$ can be expanded around k to obtain an approximate solution,

$$\beta R\simeq kR-\Gamma^c/\Delta\omega, \tag{5.12}$$

which can be easily verified by substituting this result into Eq. (5.9). Figure 8 shows the uncoupled waveguide band, the split waveguide bands around ω_0 calculated from Eq. (5.11), and the photonic bands obtained from the above asymptotic approximation. It is interesting to notice that the asymptotic approximation actually gives a fairly good description of the indirect CROW bands.

In closing this section, we remark that if $\cos(k_0R)\simeq\pm1$ it is possible that one of the split bands becomes extremely flat. This scenario is illustrated in Fig. 9, where $k_0R=3.0$ and $R\Gamma^c/v_g=0.05$. The nearly horizontal band lies close to the resonance frequency $\omega=\omega_0$. The flatness of the band indicates extremely low propagating group velocity. The group velocity is reduced to a large extent due to the fact that, when propagating through the indirect CROW structure, photons are trapped inside the resonance cavities most of the time. This property may find applications when low photon propagating velocity is desired, such as in the case of band edge lasers [37].

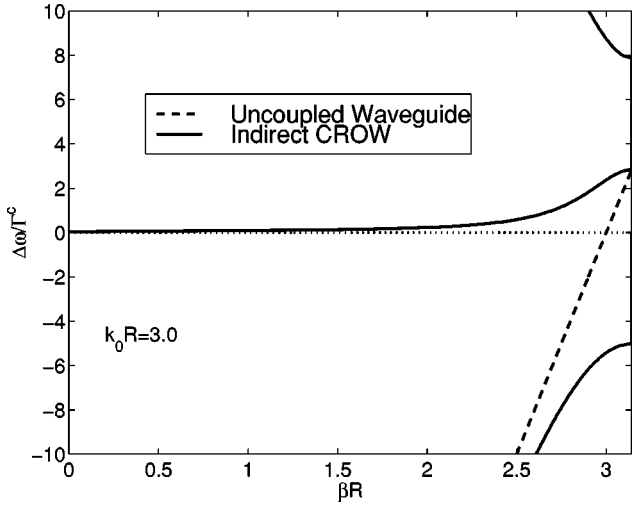

FIG. 9. Near horizontal indirect CROW band. Photon group velocity is greatly reduced for the middle band shown above. The dashed line is the unperturbed waveguide band. We use $k_0R=3.0$ and $R\Gamma^c/v_g=0.05$.

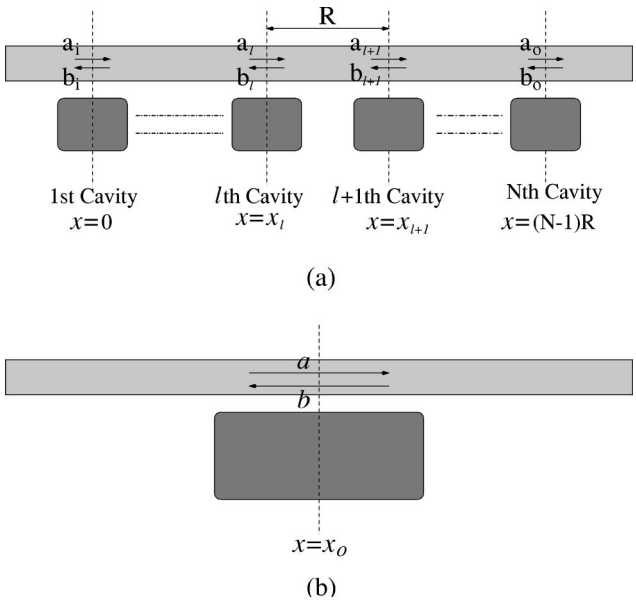

FIG. 10. (a) A straight waveguide side coupled to N resonators. The incident optical wave is described by $[a_i b_i]$; the output optical wave is given by $[a_o b_o]$. (b) A straight waveguide coupled to a resonator that possesses mirror reflection symmetry with respect to the plane $x=x_o$.

VI. OPTICAL TRANSMISSION AND REFLECTION THROUGH A WAVEGUIDE COUPLED WITH MULTIPLE CAVITIES

We have discussed the light reflection and transmission characteristics of some simple coupled waveguide-resonator systems in Sec. IV. Yet it is of both theoretical and practical interest to investigate more complicated geometries. As an example, Fig. 10(a) shows a structure composed of N identical resonators periodically side coupled to a straight waveguide. To simplify our analysis, we assume that each resonator is single mode and possesses mirror reflection symmetry.

First we reconsider the case where a straight waveguide is coupled to a single cavity. As shown in Fig. 10(b), we choose the origin of the x coordinate such that $x=x_o$ is the mirror reflection symmetry plane of the system. As before, we express the propagating waveguide mode as

$$\psi(\vec{r})=ae^{ik(x-x_o)}u_k(\vec{r})+be^{-ik(x-x_o)}u_{-k}(\vec{r}), \qquad (6.1)$$

where we choose the wave function of the propagating mode such that under the mirror reflection operation $x-x_o\rightarrow-(x-x_o)$

$$\mathbf{O}_{x=x_o}[e^{ik(x-x_o)}u_k(\vec{r})]=e^{-ik(x-x_o)}u_{-k}(\vec{r}), \qquad (6.2)$$

where the operator $\mathbf{O}_{x=x_o}$ represents the mirror reflection with respect to the plane $x=x_o$. Using the same matrix formalism as in the previous section, from Eq. (3.6), we know that if the wave to the left of the resonator is described by $[1\ \ r]$, then the wave to the right is given by $[t\ \ 0]$. On the other hand, if the wave to the right is $[r\ \ 1]$, the mirror reflection symmetry dictates that the wave to the left must be $[0\ \ t]$. Since the two waves can be related to each other via matrix $\mathbf{M}$, we have

$$\begin{bmatrix} t \\ 0 \end{bmatrix}=\mathbf{M}\begin{bmatrix} 1 \\ r \end{bmatrix},\quad \begin{bmatrix} r \\ 1 \end{bmatrix}=\mathbf{M}\begin{bmatrix} 0 \\ t \end{bmatrix}, \qquad (6.3)$$

which gives

$$\mathbf{M}=\begin{bmatrix} \dfrac{t^2-r^2}{t} & \dfrac{r}{t} \\ -\dfrac{r}{t} & \dfrac{1}{t} \end{bmatrix}. \qquad (6.4)$$

When we study the case of a waveguide coupled to N identical resonators as shown in Fig. 10(a), the scattering by each resonator can still be described by the matrix $\mathbf{M}$ as given by Eq. (6.4). However, to apply Eq. (6.4) to describe the lth resonator, we need to choose x_o in Eq. (6.2) as x_l. Therefore, if the same $\mathbf{M}$ matrix is used to describe the next resonator, we should switch to another basis of wave functions where x_o is $x_{l+1}=x_l+R$. Consequently, we have

$$\begin{bmatrix} a_{l+1} \\ b_{l+1} \end{bmatrix}=\mathbf{D}\begin{bmatrix} a_l \\ b_l \end{bmatrix}, \qquad (6.5a)$$

$$\mathbf{D}=\begin{bmatrix} e^{ikR} & 0 \\ 0 & e^{-ikR} \end{bmatrix}\begin{bmatrix} \dfrac{t^2-r^2}{t} & \dfrac{r}{t} \\ -\dfrac{r}{t} & \dfrac{1}{t} \end{bmatrix}. \qquad (6.5b)$$

It should be remembered that the wave function basis for $[a_{l+1}\ \ b_{l+1}]$ is *different* from that for $[a_l\, b_l]$.

Assuming that the center of the first resonator is located at $x=0$, we choose the wave function basis according to Eq. (6.1) with $x_o=0$. In the *same* wave function basis, the output optical wave $[a_o\ \ b_o]$ after the Nth resonator is related to the incident wave $[a_i\ \ b_i]$ through

$$\begin{bmatrix} a_o \\ b_o \end{bmatrix}=\begin{bmatrix} e^{-iNkR} & 0 \\ 0 & e^{iNkR} \end{bmatrix}\mathbf{D}^N\begin{bmatrix} a_i \\ b_i \end{bmatrix}. \qquad (6.6)$$

We consider the simplest case where the cavity possesses mirror reflection symmetry and supports only a single mode, where r can be found from Eq. (3.6),

$$r=\frac{-i}{\Delta\omega+i(\Gamma^0+\Gamma^c)}\frac{L}{v_g}V_{-k,n}V_{n,k}. \qquad (6.7)$$

Assuming that the parity of the cavity mode is given by P, from Eq. (2.4), we have

$$V_{-k,n}=PV_{k,n}. \qquad (6.8)$$

Using this relation, Eq. (6.7) is simplified as

$$r=-i\frac{P\Gamma^c}{\Delta\omega+i(\Gamma^0+\Gamma^c)}. \tag{6.9}$$

The transmission coefficient is

$$t=\frac{\Delta\omega+i\Gamma^0}{\Delta\omega+i(\Gamma^0+\Gamma^c)}. \tag{6.10}$$

Substituting Eq. (6.9) and Eq. (6.10) into Eq. (6.5b), we find

$$\mathbf{D}=\frac{1}{\Delta\omega+i\Gamma^0}\begin{bmatrix} e^{ikR}[\Delta\omega+i(\Gamma^0-\Gamma^c)] & -iP\Gamma^c e^{ikR} \\ iP\Gamma^c e^{-ikR} & e^{-ikR}[\Delta\omega+i(\Gamma^0+\Gamma^c)] \end{bmatrix}. \tag{6.11}$$

To find the reflection and transmission coefficients, we calculate $\mathbf{D}^N$ by using the procedure in Ref. [38]. First we obtain the eigenvalue equation of matrix $\mathbf{D}$:

$$\lambda^2-2\lambda\left[\cos(kR)+\frac{\Gamma^c}{\Delta\omega+i\Gamma^0}\sin(kR)\right]+1=0. \tag{6.12}$$

Then we use the Hamilton-Cayley theorem [39], which says that the matrix obeys the same equation as its eigenvalue equation,

$$\mathbf{D}^2-2\mathbf{D}\left[\cos(kR)+\frac{\Gamma^c}{\Delta\omega+i\Gamma^0}\sin(kR)\right]+1=0. \tag{6.13}$$

Thus, if we define β as

$$\cos(\beta R)=\cos(kR)+\frac{\Gamma^c}{\Delta\omega+i\Gamma^0}\sin(kR), \tag{6.14}$$

we find [39]

$$\mathbf{D}^N=\mathbf{D}\frac{\sin(N\beta R)}{\sin(\beta R)}-\mathbf{I}\frac{\sin(N-1)\beta R}{\sin(\beta R)}, \tag{6.15}$$

where $\mathbf{I}$ is the identity matrix.

With the optical amplitude at the input and output given by Eq. (6.6) and the expression for $\mathbf{D}^N$ given by Eq. (6.15), we can easily evaluate the optical transmission and reflection coefficients due to the presence of N resonators. The results in general depend critically on the values of $\Delta\omega$, Γ^0/Γ^c,N, and k_0R. However, under the condition of $\Delta\omega=0$ and $k_0R=n\pi$, the optical transmission and reflection coefficients are of simple form. In this case, $\mathbf{D}$ and $\mathbf{D}^N$ can be evaluated as

$$\mathbf{D}=(-1)^n\begin{bmatrix} 1-\frac{\Gamma^c}{\Gamma^0} & -P\frac{\Gamma^c}{\Gamma^0} \\ P\frac{\Gamma^c}{\Gamma^0} & 1+\frac{\Gamma^c}{\Gamma^0} \end{bmatrix}, \tag{6.16}$$

and

$$\mathbf{D}^N=(-1)^{Nn}\begin{bmatrix} 1-\frac{N\Gamma^c}{\Gamma^0} & -P\frac{N\Gamma^c}{\Gamma^0} \\ P\frac{N\Gamma^c}{\Gamma^0} & 1+\frac{N\Gamma^c}{\Gamma^0} \end{bmatrix}. \tag{6.17}$$

The power transmission and reflection coefficients of the whole system can readily be calculated as

$$T=\frac{1}{(1+N\Gamma^c/\Gamma^0)^2},\quad R=\left[\frac{N\Gamma^c/\Gamma^0}{1+N\Gamma^c/\Gamma^0}\right]^2. \tag{6.18}$$

It is evident from Eq. (6.18) that under the condition of $k_0R=n\pi$ the resonant transmission and reflection characteristics of a waveguide coupled to N equally spaced single mode resonators each with intrinsic loss Γ^0 are the same as if the waveguide is coupled to a *single* resonator with intrinsic loss Γ^0/N, which was analyzed in Sec. IV. In general, however, such a scaling property with respect to N does not hold for arbitrary values of $\Delta\omega$ and k_0R. In the rest of this section, we shall use Eq. (6.6), Eq. (6.14), and Eq. (6.15) to find the transmission and reflection properties of such coupled waveguide-resonator systems. The parameter β as defined in Eq. (6.14) is very similar to the Bloch wave vector of the

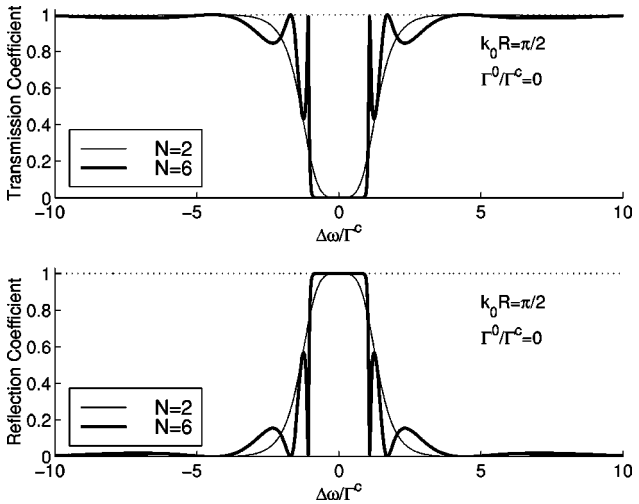

FIG. 11. The transmission and reflection coefficients of a straight waveguide side coupled to N resonators, with $N=2$ and $N=6$, respectively. $\Gamma^0/\Gamma^c=0$ and $k_0R=\pi/2$ are used in the calculations. As in the previous calculations of band structures, $R\Gamma^c/v_g=0.05$.

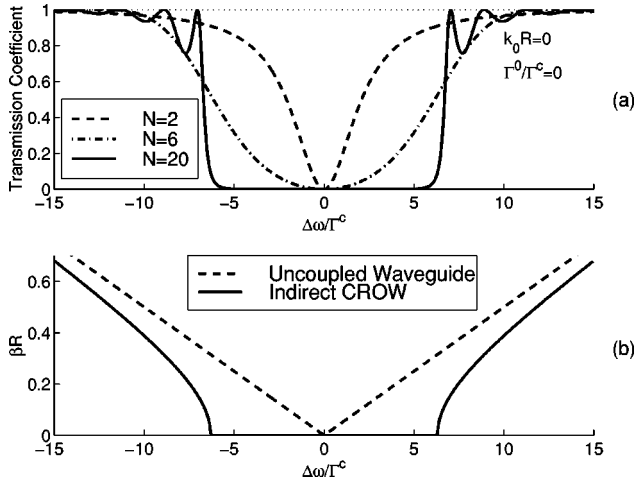

FIG. 12. (a) The transmission spectrum of a straight waveguide side coupled to N resonators, with $N=2,N=6$, and $N=20$, respectively. $\Gamma^0/\Gamma^c=0,k_0R=0$, and $R\Gamma^c/v_g=0.05$ are used in the calculations. (b) The photonic band of a straight waveguide side coupled to an infinite array of resonators like those in (a). The band structures are calculated using Eq. (5.11), with $k_0R=0$ and $R\Gamma^c/v_g=0.05$. It is clear that the band gap in (b) corresponds to the transmission dip for the case of $N=20$ in (a).

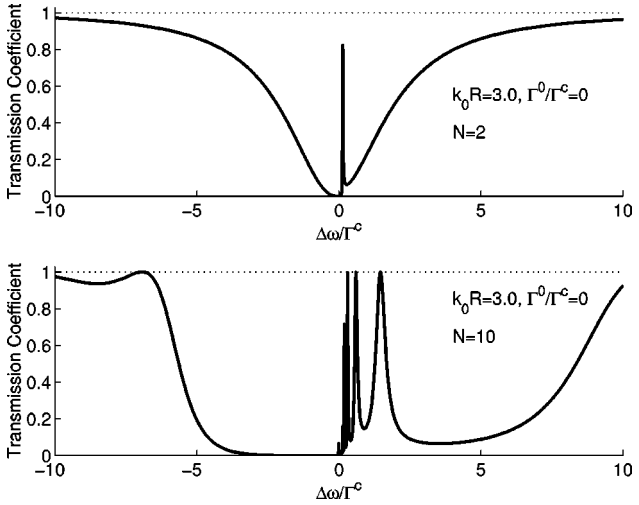

FIG. 13. The transmission spectrum of a straight waveguide side coupled to N resonators, with $N=2$ and $N=10$, respectively. We consider the case of $\Gamma^0/\Gamma^c=0$ and $k_0R=3.0$. As in the previous calculations, $R\Gamma^c/v_g=0.05$.

compound waveguide in the previous section and can be calculated using the same assumption of linear dispersion. In all the calculations of β, we choose the same $R\Gamma^c/v_g=0.05$.

In Fig. 11, we show the transmission and reflection spectra for a waveguide coupled to $N=2$ and $N=6$ resonators. We assume that there is no loss or gain and $k_0R=\pi/2$. It is interesting to notice that for only two resonators the transmission dip and the reflection peak are no longer Lorentzian and relatively flat. For the case of $N=6$, the transmission dip around $\Delta\omega=0$ becomes extremely flat. We also observe the rapid oscillation of the transmission coefficient around the transmission dip, which is caused by the optical interference between the six resonators.

In Fig. 12(a), we assume that $k_0R=0,\Gamma^0/\Gamma^c=0$ and show the transmission spectrum for a waveguide coupled to $N=2,N=6$, and $N=20$ cavities. It is interesting to notice that only the case of $N=20$ resonators produces a flat transmission dip. In Fig. 12(b), we show the photonic bands in the indirect CROW that corresponds to the coupled waveguide-resonator system in Fig. 12(a). We notice that the band gap in the indirect CROW corresponds exactly to the transmission dip of $N=20$ resonators in Fig. 12(a). It is interesting that in Fig. 11 ($k_0R=\pi/2$), it takes only six resonators to produce a flat transmission dip, while under the condition of $k_0R=0$ it requires 20 resonators.

We have observed in the previous section that it is possible to create a very flat photonic band close to $\Delta\omega=0$ in an indirect CROW (see Fig. 9, where $k_0R=3.0$ is used). We use the same value of k_0R to evaluate the optical transmission through a waveguide coupled to N lossless resonators, with N equal to 2 and 10. The results are shown in Fig. 13. For the case of $N=2$, we observe the presence of a narrow transmission peak around $\Delta\omega=0$. For $N=10$, multiple high transmission peaks are formed within the frequency range of $0<\Delta\omega/\Gamma^c<2.5$, which roughly corresponds to the flat CROW band observed in Fig. 9. The appearance of multiple peaks instead of a plateau of high transmission is likely due to the imperfect coupling between the unperturbed waveguide band and the flat CROW band.

In Sec. IV, we found that the optical transmission and reflection depend critically on the cavity loss (gain). For a waveguide coupled to multiple resonators, we expect to see similar critical dependence. In Fig. 14, we calculate the optical transmission and reflection coefficients of a waveguide coupled to six resonators, with $k_0R=\pi/2$ and $R\Gamma^c/v_g=0.05$. In the presence of cavity loss, we find that the rapid oscillation of the transmission coefficient vanishes around the edge of the transmission dip. This is due to the reduced interference between the lossy resonators. When cavity gain is introduced, we find that the transmission and reflection are greatly enhanced at frequencies corresponding to the band edge of the indirect CROW band as shown in Fig. 7. This gain enhancement is a direct consequence of the slow group

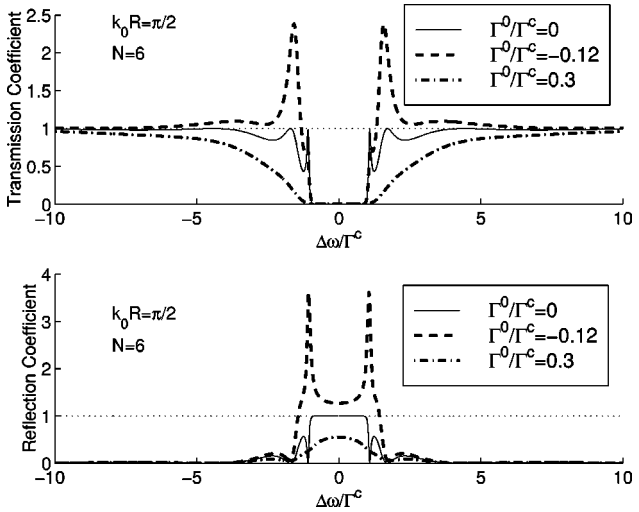

FIG. 14. The transmission and reflection spectra of a waveguide coupled to N resonators with loss ($\Gamma^0/\Gamma^c>0$) or gain ($\Gamma^0/\Gamma^c<0$). We use $N=6,k_0R=\pi/2$, and $R\Gamma^c/v_g=0.05$ in the calculations.

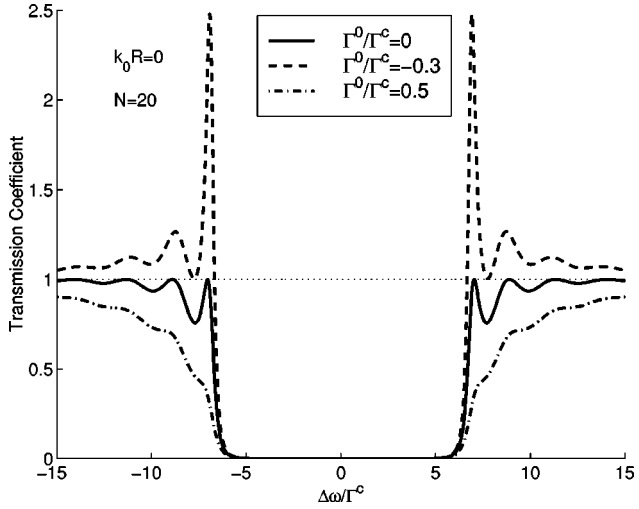

FIG. 15. The transmission spectrum of a waveguide coupled to 20 resonators with loss or gain. $k_0R=0$ and $R\Gamma^c/v_g=0.05$ are used in the calculations.

velocity at the edge of the indirect CROW band. In Fig. 15, where $N=20$ and $k_0R=0$, we also find a diminished transmission side lobe in the presence of cavity loss, and sharp enhancement of optical transmission at the band edge when the cavities possess gain. However, comparing Fig. 15 to Fig. 14, we observe that it takes more cavities to obtain the same amount of optical enhancement when $k_0R=0$. Finally, we study the case of $N=6$ and $k_0R=3.0$, which is shown in Fig. 16. With the presence of cavity loss $\Gamma^0/\Gamma^c=0.3$, we find that the transmission peaks around $\Delta\omega=0$ in the case of lossless cavities are greatly reduced. With cavity gain $\Gamma^0/\Gamma^c=-0.12$, we find a sharp peak of enhanced optical transmission close to $\Delta\omega=0$. Indeed, comparing Fig. 16 to Fig. 14, we find that the enhancement of the optical transmission for $k_0R=3.0$ is much larger than the case of $k_0R=\pi/2$. As a concluding remark, we observe that the phenomenon of effective gain enhancement is a direct consequence of the reduced group velocity around the band edge [38].

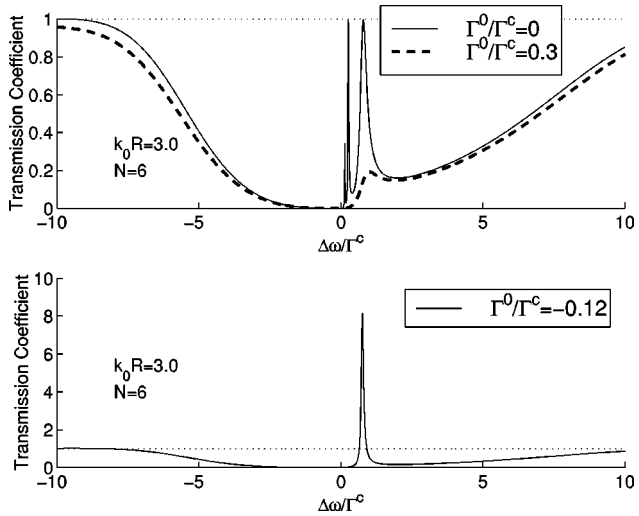

FIG. 16. The transmission spectrum of a waveguide coupled to six resonators. $k_0R=3.0$ and $R\Gamma^c/v_g=0.05$ are used in the calculations.

VII. SUMMARY

We generalize the scattering-theory formalism to discuss the coupling between waveguides and high Q optical resonators possessing loss or gain. We calculate the optical transmission and reflection coefficients for two basic coupling geometries, the side coupling geometry and the resonant coupling geometry. It is found that the optical transmission and reflection characteristics depend critically on the the coupling between the waveguide and the resonator, the degeneracy of the cavity modes, and the cavity loss or gain. We propose the concept of an indirect CROW formed by coupling an infinite array of high Q optical resonators to a straight waveguide. The dispersion relation of the indirect CROW bands is calculated using a matrix formalism based on scattering-theory results. Finally, we derive an analytical formula that gives the optical transmission and reflection coefficients for a waveguide coupled to N identical optical resonators. Using this result, we discuss the dependence of the optical transmission and reflection characteristics on various cavity and waveguide parameters.

ACKNOWLEDGMENTS

This research was sponsored by the Air Force Office of Scientific Research and the Office of Naval Research. R.K.L. also acknowledges support from the National Science and Engineering Research Council of Canada.

APPENDIX A

To derive Eq. (2.6), we first use Eq. (2.5) and express the term $\mathbf{T}|k_i\rangle$ as the sum of an infinite series,

$$\mathbf{T}|k_i\rangle=\left[\sum_{l=0}^{\infty}\left(\frac{1}{\omega_{k_i}-\mathbf{H}_0+i\epsilon}\mathbf{V}\right)^l\right]|k_i\rangle. \tag{A1}$$

We define the renormalized Green function $\mathbf{G}$ as

$$G_{m,n}(\omega)=\langle m|\mathbf{G}|n\rangle = \left\langle m\left|\sum_{l=0}^{\infty}\frac{1}{\omega-\mathbf{H}_0+i\epsilon}\left(\mathbf{V}\frac{1}{\omega-\mathbf{H}_0+i\epsilon}\right)^l\right|n\right\rangle. \tag{A2}$$

Multiplying Eq. (A1) from the left by $|k_j\rangle$ and using the above definition for $\mathbf{G}$, we find

$$T_{k_j,k_i}=\langle k_j|\mathbf{T}|k_i\rangle=\delta_{k_j,k_i} + \frac{1}{\omega_{k_i}-\omega_{k_j}+i\epsilon}\sum_{m,n}V_{k_j,m}G_{m,n}(\omega_{k_i})V_{n,k_i}, \tag{A3}$$

which is exactly Eq. (2.6a). Equation (2.6b) can also be proved in a similar way.

We notice that for any matrix $\mathbf{A}$ with all its eigenvalues less than 1, we have the identity

$$\frac{1}{\mathbf{I}-\mathbf{A}}=\sum_{l=0}^{\infty}\mathbf{A}^l, \tag{A4}$$

where **I** is a unit matrix. Applying this relation to Eq. (A2), we find

$$\mathbf{G}=\frac{1}{\omega-\mathbf{H}_0+i\epsilon}\sum_{l=0}^{\infty}\left(\mathbf{V}\frac{1}{\omega-\mathbf{H}_0+i\epsilon}\right)^l$$
$$=\frac{1}{\omega-\mathbf{H}_0+i\epsilon}\frac{1}{\mathbf{I}-\mathbf{V}/(\omega-\mathbf{H}_0+i\epsilon)}$$
$$=\frac{1}{\omega-\mathbf{H}+i\epsilon}, \tag{A5}$$

where we have used the relation $\mathbf{H}=\mathbf{H}_0+\mathbf{V}$.

APPENDIX B

In order to derive Eq. (2.7), we start by rewriting Eq. (A2) as

$$G_{n_2,n_1}=\langle n_2|\mathbf{G}|n_1\rangle=\frac{1}{\omega-\Omega_{n_1}+i\epsilon}\sum_{l=0}^{\infty}a^l_{n_2,n_1}, \tag{B1a}$$

$$a^l_{n_2,n_1}=\langle n_2|\mathbf{A}_l|n_1\rangle=\left\langle n_2\left|\left(\frac{1}{\omega-\mathbf{H}_0+i\epsilon}\mathbf{V}\right)^l\right|n_1\right\rangle, \tag{B1b}$$

where the indices n_2 and n_1 refer to the optical modes within the high Q resonator, and Ω_{n_1} is the frequency of mode $|n_1\rangle$ as given by the unperturbed Hamiltonian $\mathbf{H}_0$.

We can express $a^l_{n_2,n_1}$ in terms of lower order terms,

$$a^l_{n_2,n_1}=\sum_{n_3}\left\langle n_2\left|\frac{1}{\omega-\mathbf{H}_0+i\epsilon}\mathbf{V}\right|n_3\right\rangle \times\left\langle n_3\left|\frac{1}{\omega-\mathbf{H}_0+i\epsilon}\mathbf{V}^{l-1}\right|n_1\right\rangle$$
$$+\sum_{k,n_3}\left\langle n_2\left|\frac{1}{\omega-\mathbf{H}_0+i\epsilon}\mathbf{V}\right|k\right\rangle\left\langle k\left|\frac{1}{\omega-\mathbf{H}_0+i\epsilon}\mathbf{V}\right|n_3\right\rangle \times\left\langle n_3\left|\frac{1}{\omega-\mathbf{H}_0+i\epsilon}\mathbf{V}^{l-2}\right|n_1\right\rangle$$
$$=\frac{1}{\omega-\Omega_{n_2}+i\epsilon}\left(\sum_{n_3}V_{n_2,n_3}a^{l-1}_{n_3,n_1}+\sum_{k,n_3}V_{n_2,k}\frac{1}{\omega-\omega_k+i\epsilon}V_{k,n_3}a^{l-2}_{n_3,n_1}\right). \tag{B2}$$

To cast this relation in a simpler form, we define the following matrix operator within the subspace expanded by the high Q modes $|n\rangle$:

$$\langle n_2|\mathbf{G}_0|n_1\rangle=\frac{\delta_{n_2,n_1}}{\omega-\Omega_{n_1}+i\epsilon}, \tag{B3a}$$

$$\langle n_2|\mathbf{V}_d|n_1\rangle=V_{n_2,n_1}, \tag{B3b}$$

$$\langle n_2|\mathbf{V}_i|n_1\rangle=\sum_k V_{n2,k}\frac{1}{\omega-\omega_k+i\epsilon}V_{k,n_1}, \tag{B3c}$$

where the terms $\mathbf{V}_d$ and $\mathbf{V}_i$ represent the direct and indirect interaction, respectively, between the cavity modes.

The matrix form of Eq. (B1) is

$$\mathbf{G}=\left(\sum_{l=0}^{\infty}\mathbf{A}_l\right)\mathbf{G}_0. \tag{B4}$$

With the initial conditions for $\mathbf{A}_l$ given by

$$\mathbf{A}_0=\mathbf{I},\ \mathbf{A}_1=\mathbf{G}_0\mathbf{V}_d, \tag{B5}$$

we find

$$\mathbf{G}=\mathbf{G}_0+\mathbf{G}_0(\mathbf{V}_d+\mathbf{V}_i)\mathbf{G}, \tag{B6}$$

where we have used the relation Eq. (B2).

Consequently, we have

$$\mathbf{G}^{-1}=\mathbf{G}_0^{-1}-(\mathbf{V}_d+\mathbf{V}_i). \tag{B7}$$

Using Eq. (B3), we find that the above equation is exactly Eq. (2.7).

[1] E. Yablonovitch, Phys. Rev. Lett. **58**, 2059 (1987).
[2] S. John, Phys. Rev. Lett. **58**, 2486 (1987).
[3] J.D. Joannopoulos, R.D. Meade, and J.N. Winn, *Photonic Crystals* (Princeton University Press, Princeton, NJ, 1995).
[4] R.D. Meade, A. Devenyi, J.D. Joannopoulos, O.L. Alerhand, D.A. Smith, and K. Kash, J. Appl. Phys. **75**, 4753 (1994).
[5] P.R. Villeneuve, S. Fan, and J.D. Joannopoulos, Phys. Rev. B **54**, 7837 (1996).
[6] R.K. Lee, O.J. Painter, B. Kitzke, A. Scherer, and A. Yariv, Electron. Lett. **35**, 569 (1999).
[7] T. Baba, N. Fukaya, and J. Yonekura, Electron. Lett. **35**, 654 (1999).
[8] M. Sigalas, C.M. Soukoulis, E.N. Economou, C.T. Chan, and K.M. Ho, Phys. Rev. B **48**, 14121 (1993).
[9] G. Tayeb, and D. Maystre, J. Opt. Soc. Am. A **14**, 3323 (1997).
[10] D.R. Smith, S. Schultz, S.L. McCall, and P.M. Platzmann, J. Mod. Opt. **41**, 395 (1994).
[11] P. Sabouroux, G. Tayeb, and D. Maystre, Opt. Commun. **160**, 33 (1999).
[12] S. Fan, P.R. Villeneuve, J.D. Joannopoulos, and H.A. Haus, Phys. Rev. Lett. **80**, 960 (1998).
[13] S. Fan, P.R. Villeneuve, J.D. Joannopoulos, M.J. Khan, C. Manolatou, and H.A. Haus, Phys. Rev. B **59**, 15 882 (1999).
[14] C. Manolatou, M.J. Khan, S. Fan, P.R. Villeneuve, H.A. Haus, and J.D. Joannopoulos, IEEE J. Quantum Electron. **35**, 1322 (1999).
[15] J. Danglot, O. Vanbésien, and D. Lippens, IEEE Microwave Guid. Wave Lett. **9**, 274 (1999).
[16] L.F. Stokes, M. Chodorow, and H.J. Shaw, Opt. Lett. **7**, 288

(1982).
[17] A. Serpengüzel, S. Arnold, and G. Griffel, Opt. Lett. **20**, 654 (1995).
[18] J.C. Knight, N. Dubreuil, V. Sandoghdar, J. Hare, V. Lefèvre-Seguin, J.M. Raimond, and S. Haroche, Opt. Lett. **21**, 698 (1996).
[19] B.E. Little, S.T. Chu, H.A. Haus, J. Foresi, and J.-P. Laine, J. Lightwave Technol. **15**, 998 (1997).
[20] F.C. Blom, D.R. van Dijk, H.J.W.M. Hoekstra, A. Driessen, and Th.J.A. Popma, Opt. Lett. **71**, 747 (1997).
[21] D. Rafizadeh, J.P. Zhang, S.C. Hagness, A. Taflove, K.A. Stair, S.T. Ho, and R.C. Tiberio, Opt. Lett. **22**, 1244 (1997).
[22] A. Yariv, Electron. Lett. **36**, 321 (2000).
[23] K. Hayata, H. Yénaka, and M. Koshiba, Opt. Lett. **18**, 1385 (1993).
[24] T. Mukaiyama, K. Takeda, H. Miyazaki, Y. Jimba, and M. Kuwata-Gonokami, Phys. Rev. Lett. **82**, 4623 (1999).
[25] M. Bayer, T. Gutbrod, J.P. Reithmaier, A. Forchel, T.L. Reinecke, P.A. Knipp, A.A. Dremin, and V.D. Kulakovskii, Phys. Rev. Lett. **81**, 2582 (1998).
[26] N. Stefanou and A. Modinos, Phys. Rev. B **57**, 12127 (1998).
[27] A. Yariv, Y. Xu, R.K. Lee, and A. Scherer, Opt. Lett. **24**, 711 (1999).
[28] Y. Xu, R.K. Lee, and A. Yariv, J. Opt. Soc. Am. B **17**, 387 (2000).
[29] See, for example, N.W. Ashcroft, and N.D. Mermin, *Solid State Physics* (Saunders College Publishing, Philadelphia, 1976).
[30] A. Mekis, J.C. Chen, I. Kurland, S. Fan, P.R. Villeneuve, and J. D. Joannopoulos, Phys. Rev. Lett. **77**, 3787 (1996).
[31] S.C. Hagness, D. Rafizadeh, S.T. Ho, and A. Taflove, J. Lightwave Technol. **15**, 2154 (1997).
[32] J. Yonekura, M. Ikeda, and T. Baba, J. Lightwave Technol. **17**, 1500 (1999).
[33] Y. Xu, R.K. Lee, and A. Yariv, Opt. Lett. **25**, 755 (2000).
[34] H.A. Haus, and Y. Lai, IEEE J. Quantum Electron. **28**, 205 (1992).
[35] J.J. Sakurai, *Modern Quantum Mechanics* (Addison-Wesley, Reading, MA, 1994).
[36] A. Yariv and P. Yeh, *Optical Waves in Crystals* (Wiley, New York, 1984).
[37] J.P. Dowling, M. Scalora, M.J. Bloemer, and C.M. Bowden, J. Appl. Phys. **75**, 1896 (1994).
[38] J.M. Bendickson, J.P. Dowling, and M. Scalora, Phys. Rev. E **53**, 4107 (1996).
[39] G.E. Shilov, *Linear Algebra* (Dover Publications, Inc., New York, 1977).